UNIVERSITAT DE BARCELONA

FACULTAT DE FÍSICA

Màster en Biofísica

Study of a two-state model for a membrane channel

Projecte final del Màster en Biofísica 2008/09 - II:
Javier G. Orlandi

Tutor: Dr. José Mª Sancho

Keywords: membrane transport, molecular channels, molecular machines, controlling membrane flux

Contents

1 Introduction **2**
1.1 Transport and membrane channels 2
1.2 The Biophysical approach to membrane channels 3
1.3 Project Outline 4

2 Models **4**
2.1 Introduction 4
2.2 Theoretical framework 5
2.3 The Free Channel 5
2.4 The White Noise Model 7
2.5 The Dichotomic Model 8
2.5.1 Transition rates: The ATP hydrolysis 10
2.5.2 Zero order approximation 10
2.5.3 Complete solution 11

3 Numerical analysis **12**
3.1 Simulation framework 12
3.2 Algorithm 12

4 Results **13**
4.1 Concentration profiles 13
4.1.1 Free Channel and White Noise Model 13
4.1.2 Dichotomic Model 14
4.2 Fluxes and conductances 14
4.2.1 Analytical 14
4.2.2 Simulation 15

5 Conclusions **19**

6 Perspectives **19**
6.1 Modeling a voltage-gated channel 20

Abstract

We explore biological transport across membrane channels from a physical point of view. The main objective is to use the tools available to a physicist from non-equilibrium thermodynamics and apply them to a concrete biological problem. In this case, we focus our attention in trying to build simple physical models, yet not trivial, that match the behavior of real channels, or ones that can be synthetically accomplished.

We start with a brief review of the results we obtained for a model with multiplicative noise [1] and proceed to study a dichotomic model, introducing a more realistic description of channel gating, both analytically and numerically. We also introduce a new different simulation framework that allows more flexibility in parameter exploration than the one previously used.

1 Introduction

1.1 Transport and membrane channels

Membrane channels are one of the two main structures[1] involved in transport across the cell membrane. They transport water or specific types of ions and hydrophilic molecules down their concentration gradient. Such transport is often called passive transport or facilitated diffusion. Channel proteins form a hydrophilic pathway across the membrane through which multiple molecules are allowed to flow through simultaneously [2, 3].

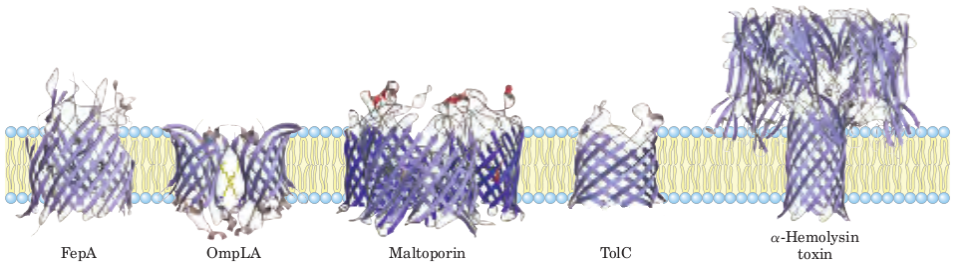

Figure 1: Different examples of membrane proteins. All of these include a β-barrel structure forming a pathway between both sides of the membrane (Ref. [2]).

Some channels are open most of the time, these are the so called non-gated channels, but most of them are usually closed, and only open after an activation signal, being that signal either an electrical stimuli (like voltage-gated channels [4]), a ligand-binding process, or simply ATP hydrolysis;

[1] The other one being pumps.

hence the name of gated channels. They are also highly selective, existing specific channels for almost any substance that needs to cross the membrane.

Although being passive transporters, channels are much more than that. While molecular pumps can transport ions and molecules at rates approaching several thousand ions per second, channels are capable of reaching speeds up to a thousand times higher, being very close to the speed of free diffusion [5]. Yet, they are not just tubes that allow diffusion across the membrane, they are sophisticated molecular machines that respond to changes in their environment and undergo precisely timed conformational changes.

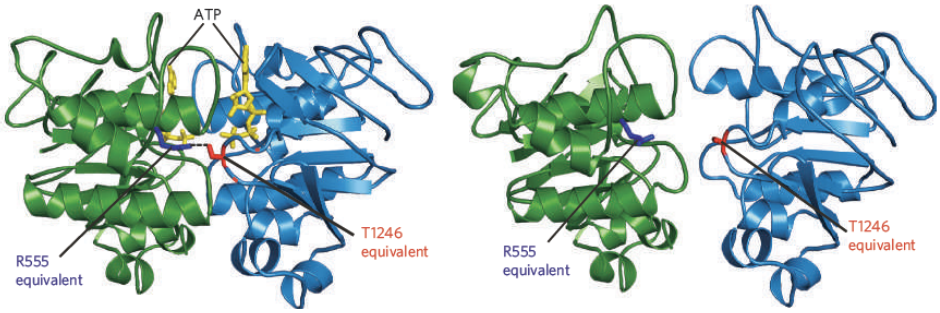

Figure 2: Cartoon representation of a membrane channel. On the left, its structure on the closed state. The binding of two ATP molecules closes the channel. On the right, the open state, no ATP is present (adapted from [6]).

1.2 The Biophysical approach to membrane channels

The introduction of the patch-clamp technique by Erwin Neher and Bert Sakmann [7] in 1976 made possible the study of single channels. With this technique one can measure the activity of a single channel. The flow of ions through a single channel and the transitions between the open and closed states of a channel can be monitored with a time resolution of microseconds. Also, the channel can be studied in its native environment, even in an intact cell. This technique, and newer ones, makes possible a quantitative analysis of channels. From this point of view, it is also important to theoretically describe the processes involved in the transport through channels, using models more accurate than simple diffusion or chemical kinetics, but still far from molecular dynamics simulations.

A good understanding of channel transport is needed from a medical point of view. One clear example is the CFTR (Cystic fibrosis transmembrane conductance regulator) chloride channel, whose failure causes cystic fibrosis [6]. Channels, which play an essential role in the nervous system, are the main target of many toxins attacking the organism, such as poisons

and venoms, that block the channels. Also, since channels govern the fastest processes in cellular transport, they are the favorite target in the drug research industry. Creating drugs and compounds that have a high affinity with channels can improve and speed up the process of drug delivery.

Theoretical models also play an important role on recent advances in the design and construction of synthetic channels and nanopores [8, 9]. Identifying and isolating the key components involved in channel transport we can, later on, produce synthetic compounds that mimic the effects of biological channels, and also change them and make them more suitable for other tasks. Applications in this field range from the biological level, for example, to replace faulty channels, to the industrial level, allowing for example, to separate substances in a solution. Properties like the high selectivity, speed, and the fact that they can be easily controlled at will, makes them specially interesting for the industry.

1.3 Project Outline

This document is structured in the following way:

In Section 2, we introduce the different models that have been under study. We start with a brief theoretical introduction of the physics behind the problem and then proceed with the models. The first model is the most simple one, the Free Channel. Next we move to the White Noise model, which was already studied in the previous report. Then we move to the dichotomic model, which is the core of this project.

In Section 3, we detail the numerical tools and the simualtion framework used to study the different models.

In section 4, we present and explain all the obtained results (for all the models). We compare the results for each model, giving special emphasis on the similarities and on the most characteristic features of each.

In sections 5 and 6, we finish by explaining the conclusions obtained in this study, and also detail a possible follow-up study.

2 Models

2.1 Introduction

In this section we introduce the different models that have been under study in the present work. All the models are created following the same procedure and under the same theoretical framework. We start with a brief theoretical review of the physics involved in this study and then analyze each of the models in detail.

The first model (Free Channel) is a purely diffusive system. The second model (White Noise) is a symmetric linear sawtooth potential with multiplicative white noise. The third and fourth models are based on a dichotomic

noise to include the effects of channel gating.

After each model has been described and solved, we compare each of them, both analytically and with numerical simulations.

2.2 Theoretical framework

Each channel is modeled as a one-dimensional symmetric potential $V(x)$ of length L. The channel is connected with two infinite particle reservoirs with fixed concentrations, ρ_0 and ρ_1.

The dynamics of particles inside the channel are governed by a Langevin equation in the overdamped regime [10, 11] (low Reynolds number)

$$\gamma \dot{x} = -V'(x,t) + g(x,t)\eta(t), \tag{1}$$

where γ is the friction coefficient (which we take $\gamma = 1$ from now on for simplicity[2]), $g(x,t)$ a function yet to be determined (but related to a possible spatial component of the noise), $\eta(t)$ a stochastic process (noise term), and $V'(x,t)$ a time dependent force. But since we are interested in statistically averaged observables we focus on the evolution of probability and its conservation [12]

$$\frac{\partial}{\partial t}P(x,t) = -\frac{\partial}{\partial x}j(x,t), \tag{2}$$

where $P(x,t)dx$ is the probability of finding one particle between x and $x + dx$ at time t, and $j(x,t)$ is the probability flux, which we will define later on, since its exact expression will depend on the model and on the interpretation [13] of the stochastic process.

Considering the global behavior of the channel as the sum of N independent single-particle processes we can safely move from probabilities $P(x,t)$ to concentrations $\rho(x,t)$ (also from probability fluxes $j(x,t)$ to particle fluxes $J(x,t)$) and forget about the probability normalization condition.

We are mostly interested in steady-state non-equilibrium solutions, in which the flux is just a constant J, and the concentration does not change in time. In that regime, we expect to relate the fluxes and the concentrations to the concentrations of the reservoirs.

2.3 The Free Channel

The most simple model for a channel is to consider it as just a hole in the membrane, in which particles can move freely. This is a too simplistic description, but we include it in here since it serves as a baseline for more complex models.

[2]The only effect friction has on this system is to change the time scale. This is equivalent to making the substitution $t' = \gamma^{-1}t$.

As stated in the introduction, the channel has a length L and connects two infinite reservoirs with concentrations ρ_0 and ρ_1. A representation of the scheme can be seen on Fig. 3.

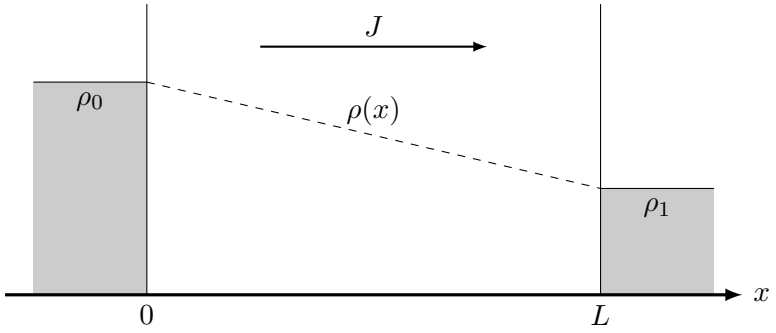

Figure 3: Structure of the free channel. The channel is modeled as a region of free diffusion against two fixed concentrations ρ_0 and ρ_1. The dashed line represents the expected density profile.

Following the previous theoretical description (1) we can model this channel as

$$\gamma\dot{x} = \eta(t), \tag{3}$$

where now $\eta(t)$ is a Gaussian white noise with autocorrelation $\langle\eta(t)\eta(t')\rangle = 2\gamma k_B T\delta(t-t')$. From the associated Fokker-Planck equation one can get the flux in the steady-state,

$$J = -\frac{k_B T}{\gamma}\frac{\partial}{\partial x}\rho(x), \tag{4}$$

whose solution (after applying boundary conditions) is

$$J = \frac{k_B T}{\gamma}\frac{\rho_0 - \rho_1}{L}, \tag{5}$$

and from the fluctuation-dissipation theorem we have that $D = k_B T/\gamma$, and the previous relation is nothing more than Fick's law for diffusion.

We can also associate the flux with a certain membrane conductance K, and to the unitary concentration 'gradient' $\phi \equiv \Delta\rho/L$

$$J = -K_0\phi, \tag{6}$$

where $K_0 = D$ is the membrane conductance associated to this model.

2.4 The White Noise Model

This is the model we developed on the first part of the project, and a detailed analysis can be found on the already published material [1]. Here we briefly review it and include new analytical results.

This model, based on the work by A. Gomez-Marin and J. M. Sancho [14], consists on a symmetric linear sawtooth potential modulated by a stochastic process. The modulation of the potential takes the form

$$V(x,t) = V(x)\left(1+\chi(t)\right), \tag{7}$$

where $\chi(t)$ is a gaussian white noise with autocorrelation $\langle\chi(t)\chi(t')\rangle = 2Q\delta(t-t')$. A scheme of the potential can be see in Fig. 4.

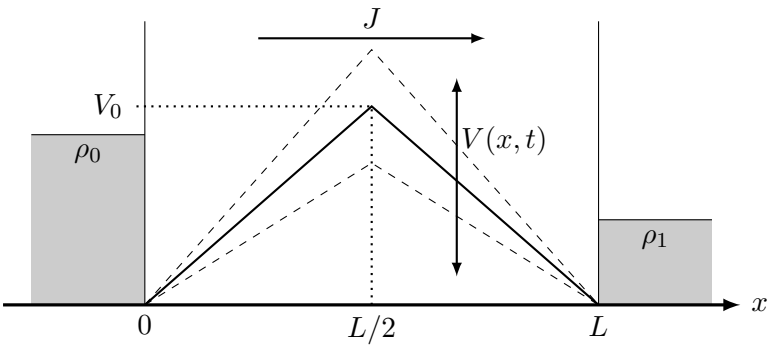

Figure 4: Structure of the white noise model. The channel is modeled as a symmetric flashing potential $V(x,t)$, the barrier height fluctuates as a white noise with strength Q.

Merging the two random processes $\eta(t)$ and $\chi(t)$ one can express the Langevin equation associated to this system as we did in (1),

$$\gamma\dot{x} = -V'(x) + g(x)\zeta(t), \tag{8}$$
$$g(x) = \sqrt{\gamma k_B T + QV'(x)^2}, \tag{9}$$

where $\zeta(t)$ is another gaussian white noise with unit variance.

Now, if we work under Itô interpretation of the stochastic process, the flux is given by [13],

$$\gamma J(x,t) = -V'P(x,t) + \frac{\partial}{\partial x}\left[g^2(x)P(x,t)\right], \tag{10}$$

and after lengthy calculations [1, 14], one finally obtains an expression for the flux as a function of the model parameters and the boundaries

$$J = \frac{k_B T}{\gamma}\frac{v}{e^v-1}\frac{\rho_0-\rho_1}{L}, \tag{11}$$

with

$$v \equiv \frac{V_0}{k_B T + 4Q\frac{V_0^2}{\gamma L^2}}, \tag{12}$$

where V_0 is the barrier height. We also introduce the dimensionless parameters $\alpha = QK_BT/(\gamma L^2)$, and $v_0 = V_0/k_BT$ for later use. We can see how the flux still depends on the concentration difference $\rho_0 - \rho_1$, but with a new factor that involves the barrier height and the noise strength. But even now, we can still express it as we did in the previous model

$$J = -K_1\phi, \tag{13}$$

$$K_1 = K_0\frac{v}{e^v - 1}, \tag{14}$$

and we can see how for very small values of V_0, and hence of v, the conductances coincide ($e^v \simeq 1 + v + O(v^2)$).

2.5 The Dichotomic Model

This model is an adaptation of the *Two-state flashing molecular pump* [15] developed by A. Gomez-Marin and J. M. Sancho, focusing on the particular case of a symmetric potential.

As with the previous models, we start with a generic Langevin description (1),

$$\gamma\dot{x} = -V'(x,t) + \eta(t), \tag{15}$$

where $V(x,t)$ now also depends on time, and $\eta(t)$ is a Gaussian white noise with autocorrelation $<\eta(t)\eta(t')>= 2\gamma k_BT\delta(t-t')$. To include the gating dynamics of the channel we model the potential as

$$V(x,t) = V(x)\zeta(t), \tag{16}$$

where $V(x)$ is a symmetric sawtooth potential of length L and height U given by (see Fig. 5),

$$\begin{aligned} V_L(x) &= \frac{2U}{L}x, & x \in (0, L/2), \\ V_R(x) &= \frac{2U}{L}(L-x), & x \in (L/2, L), \end{aligned} \tag{17}$$

and $\zeta(t)$ is a stochastic variable that can take the values $\zeta_0 = 0$ and $\zeta_1 = 1$. This stochastic variable represents the open (ζ_0) and closed (ζ_1) states of the channel, since the barrier $V(x)$ is only present in the closed state. The variable switches from one state to the other with rates ω_0 (open to closed)

and ω_1 (closed to open). This corresponds to the well known dichotomic Markov process [12, 16] with mean value and autocorrelation

$$\langle \zeta(t) \rangle = \frac{\omega_1}{\omega_0 + \omega_1}, \tag{18}$$

$$\langle \Delta\zeta(t)\Delta\zeta(t') \rangle = \frac{\omega_0\omega_1}{(\omega_0+\omega_1)^2} \exp\left(-(\omega_0+\omega_1)\left|t-t'\right|\right), \tag{19}$$

where $\Delta\zeta(t) \equiv \zeta(t) - \langle\zeta(t)\rangle$. A scheme of the whole system can be seen in Fig. 5.

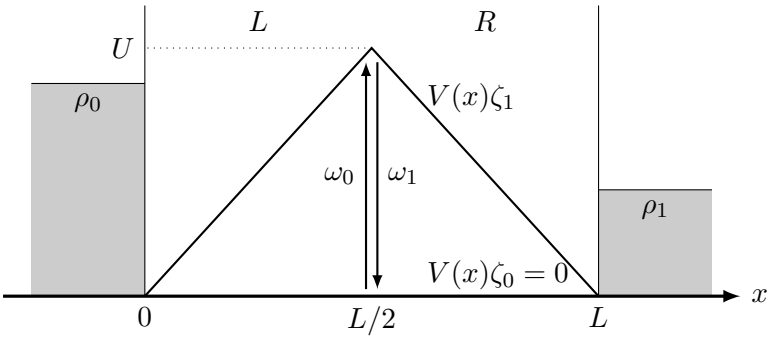

Figure 5: Structure of the channel. The channel is modeled as a two state potential $V(x)\zeta_i$ flipping between open and closed states with rates ω_i, and working between fixed concentrations ρ_0 and ρ_1.

As with the other models, now we use the continuous representation of the system. Being P_i and J_i the probabilities and fluxes associated to the state i we can write [16]

$$\begin{aligned} \partial_t P_0 + \partial_x J_0 &= -\omega_0 P_0 + \omega_1 P_1, \\ \partial_t P_1 + \partial_x J_1 &= \omega_0 P_0 - \omega_1 P_1, \end{aligned} \tag{20}$$

which is just the total conservation of probability. The creation and destruction of probability in any state ($\partial_t P_i + \partial_x J_i \neq 0$) can only happen due to the probability coming from or leaving to the other state[3]. The fluxes J_i have to satisfy the associated Fokker-Planck equation

$$J_i = -\frac{1}{\gamma}\left(k_B T \partial_x P_i + P_i V_i'(x)\right), \tag{21}$$

although this set of equations can already be solved analytically, the result is quite cumbersome, involving third order non-homogeneous differential equations [15].

[3]In other words, the Master equation for a closed two state system

2.5.1 Transition rates: The ATP hydrolysis

Until now we haven't said anything about how we model the transition rates. We consider the channel gating process to be governed by an enzymatic reaction, in which the channel is the enzyme, ATP the substrate and ADP the product. We consider the channel to open upon ATP binding to the channel, and to close after ATP hydrolysis and unbinding [6]. We model the process via Michaelis-Menten kinetics [17] such that the opening rate can be expressed as

$$\omega_1 = \omega_0 \frac{[ATP]}{k_M + [ATP]} = \frac{\omega_0}{1 + 1/\sigma}, \tag{22}$$

where ω_0 is the closing rate. We can see that the only relevant parameters are the closing rate ω_0 and the ratio between ATP concentration and the Michaelis-Menten constant $\sigma \equiv [ATP]/k_M$. This is a good model to introduce the fact that the rate of the reaction is known to saturate with increase of substrate (ATP) concentration. Hence, ω_1 is always bound by ω_0. Although the Michaelis-Menten kinetics model is based on the Mass Action Law, we consider it to be still valid for our stochastic description.

Figure 6: Experimental data showing a single channel state evolution (open/closed) in time (adapted from [6]).

2.5.2 Zero order approximation

Now we perform what we call the zero order approximation. We consider that the channel can still be in its two states, open and closed. While open, particles diffuse freely, but when the channel is closed, now we consider that the particles have completely stopped moving, rendering the whole system inactive. This approximation corresponds to the full dichotomic model when the mean-life of the states is much larger than the time it takes a particle to diffuse inside the channel. In this limit, the fluxes are

$$J_0 = -\frac{1}{\gamma} k_B T \partial_x P_0, \tag{23}$$

$$J_1 = 0, \tag{24}$$

so $J \equiv J_0 + J_1 = J_0$. Looking back at eq. (20) we see that in the steady state we have

$$P_1(x) = \frac{\omega_0}{\omega_1} P_0(x). \tag{25}$$

If we now integrate eq. (24) we obtain

$$P_0(x) = -J\frac{\gamma}{k_B T}x + C, \tag{26}$$

where C is a constant yet to be determined. If we now impose $P(0) \equiv P_0(0) + P_1(0) = \rho_0$ and combine eqs. (25) and (26) we find

$$C = \rho_0 \frac{\omega_1}{\omega_0 + \omega_1}, \tag{27}$$

and from this relation we obtain the final solution

$$J = \frac{k_B T}{\gamma}\frac{\rho_0 - \rho_1}{L}\frac{\omega_1}{\omega_0 + \omega_1}. \tag{28}$$

Proceeding as with the other models we get

$$J = -K_2\phi, \tag{29}$$

$$K_2 = K_0\frac{\omega_1}{\omega_0 + \omega_1}, \tag{30}$$

which can also be expressed in terms of ATP by using eq. (22)

$$K_2 = K_0\frac{\sigma}{1 + 2\sigma}. \tag{31}$$

We can again see the similarities with the previous models, but now the flux is modulated by the rates, in such a way that the flux is the flux of the free channel times the fraction of time the channel is open.

2.5.3 Complete solution

As we have previously stated, a solution for the complete model can be solved analytically [15]. But it is quite cumbersome, at the end one has to deal with a system of third order differential equations that involve solving a 7×7 linear system.

Instead of going that path, we will focus on the next section on implementing a simulation framework for this system (and similar ones), which was not done in [15], and is the natural continuation.

3 Numerical analysis

3.1 Simulation framework

When we studied the white noise model [1] we implemented a simulation framework based on the introduction of additional elements to the channel. Creating a closed (periodic boundary condition) system consisting of the channel, a pump (modeled as a constant force) and big reservoirs we managed to create fluxes and were able to study the behavior of the channel.

The main problem we encountered with the previous framework was that by closing the system, we could not study the fluxes at will. Closing the system means imposing a new boundary condition, and thus, varying any parameter of the system, implies a change both in fluxes and concentrations at the same time.

The new approach to simulating the system consists on eliminating most of the external setup. We only keep small reservoirs at both ends of the channel, and we impose a fixed number of particles inside each reservoir at (almost) any given time. We keep the reservoirs small enough so that it can be considered as a zone of constant concentration, but we still keep them wide enough so that particles are able to diffuse freely for some time steps.

Although the introduction of reservoirs might not seem optimal, as compared to a pure particle injection [18], it already prevents the formation of spurious boundaries while keeping the simulation simple enough that we do not need to know the full probability distribution of the system beforehand.

3.2 Algorithm

For the dynamics of the particles we proceed as we did in the previous study. Instead of using complex stochastic algorithms [19, 20], we are going to stick with Euler's first order expansion [21], since it already works quite well, and in some models, we are dealing with non-standard noises.

Integrating eq. (1) between t and $t + dt$ we obtain [4]

$$x(t + dt) = x(t) - V'[x(t)]dt + g[x(t)]X(t), \tag{32}$$

where $X(t)$ is the numerical representation of the stochastic integral

$$X(t) = \int_t^{t+dt} \eta(t')dt' = \sqrt{2dt}\alpha, \tag{33}$$

where α is a random number sampled from a normal distribution with zero mean and unit variance (the function $g(x)$ already carries the strength of the noise).

The previous algorithm is for the dynamics of the particles, but in the dichotomic model we also need to simulate the opening and closing of the

[4] We eliminate the friction again, $t' = \gamma^{-1}t$.

channel. Simulating the dynamics of the transition rates is quite straight forward, since they are always the same and do not change in time. We only need to calculate the time that will take the channel to change state with an exponential distribution with mean ω_i^{-1}, and update accordingly. In the same way as one does with the Gillespie algorithm [22, 23] for chemical kinetics. Basically we proceed as follows: let's consider that at $t = 0$ we are in state i, then we calculate the time to jump from this state[5] by choosing a random number from an exponential distribution with mean ω_i^{-1}

$$P(t) = \omega_i e^{\omega_i t}, \tag{34}$$

which can be generated from a uniform distribution $X \in [0, 1)$ with the transform

$$t_r = -\frac{\log X}{\omega_i}, \tag{35}$$

or in our case, via the ziggurat algorithm [24]. Also lets call the obtained time t_r. Then we keep running the simulation for the particles until time t_r, in which we change the channel's state and again calculate the time to the next transition.

4 Results

4.1 Concentration profiles

In this section we show the first and most basic results of the simulations, the concentration profiles in a steady state.

4.1.1 Free Channel and White Noise Model

The concentration profile for the Free Channel is already well known, and it is linear between the fixed concentrations. On Fig. 7 we show all the concentration profiles stacked. As we can see, for the free channel, we obtain pure diffusion.

For the concentration profile of the white noise model, it is clear the big difference respect to the free channel. Now the concentration decays exponentially as it goes further inside the channel. The discontinuities on the boundaries are to be expected, and are fully explained in the previous report. The discontinuities appear because the function $g(x)$ takes different values inside and outside the channel.

[5] Since we only have two states, we define the rate ω_i as the rate to leave i.

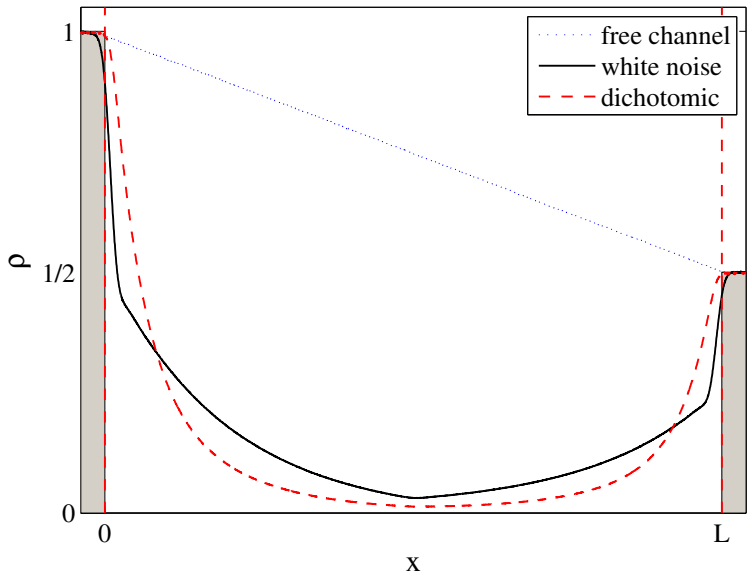

Figure 7: Simulation output for the concentration profiles associated to the different models, $\rho_1/\rho_0 = 1/2$.

4.1.2 Dichotomic Model

For the dichotomic model we only simulate the complete version, since the results associated with the zero order approximation are the same ones as with free diffusion, but with a different conductance. As we can see on its profile, (still on Fig. 7), it is similar to the one from the white noise model, but now there are no discontinuities, and the profile is smoother in the boundaries.

4.2 Fluxes and conductances

Now we study the flux dependence with the different parameters of the models: concentrations, barriers, noises, etc. We start with the analytical results we've previously obtained, and then we compare them with the simulation for the complete dichotomic model.

4.2.1 Analytical

As we have seen in the previous section, all the fluxes depend linearly with the concentration difference. So for now, we forget about the concentrations and focus on the conductances. The first interesting result can be seen on Fig. 8, where we plot the conductances for the zero order dichotomic model and the white noise model.

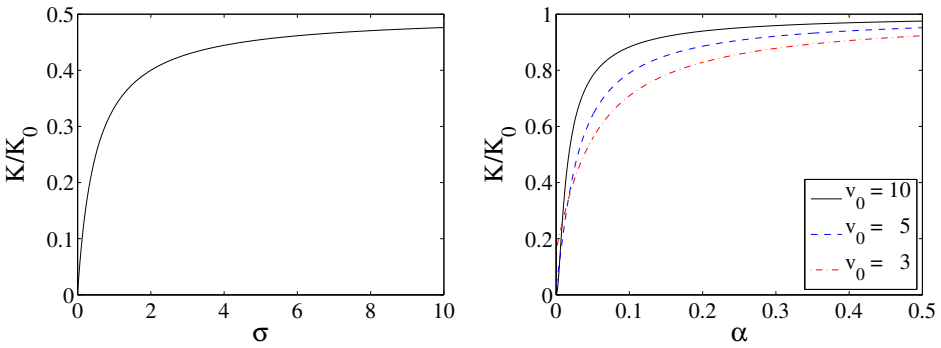

Figure 8: Left figure: Normalized conductance against $\sigma = [ATP]/k_M$ (zero order dichotomic model). Right figure: Normalized conductance against $\alpha = QK_BT/(\gamma L^2)$ (white noise model).

It is clear from the plots that the ATP concentration and the noise strength ($Q \propto \alpha$) have the same effect on the flux. An increase on them also implies an increase on the flux, until it saturates.

This result is easily understood in the dichotomic model. Basically, when there are small quantities of ATP, that is the limiting factor on the channel gating, and heavily influences the flux. But when the ATP concentration is high, the system saturates, and now the limiting factor becomes the intrinsic rate of the system. For the dichotomic model, when it saturates the flux is half the one from free diffusion, since the channel is open half the time.

The result obtained in the white noise model is harder to interpret from a gating point of view. Basically what is happening is that for small values of the noise, all the particles can see is a barrier, and the flux is small. But when the strength is large, the barrier can fluctuate so heavily that it basically becomes useless, and the flux saturates to the values of free diffusion.

4.2.2 Simulation

Now we focus exclusively on the complete dichotomic model and the simulation results. The first thing we need to check is that the fundamental relation of flux being proportional to the concentration's gradient still holds. The results are shown on Fig. 9. It is clear that the linear relation between flux and concentration gradient is still valid.

Another result that is worth checking again is the dependence of the flux with the ATP concentration, to see if the result is compatible with the one obtained from the zero order approximation. It can be seen on Fig. 10. The different curves on the figure correspond to different simulation parameters, the difference being the barrier height V_0. It is smaller for the red curve

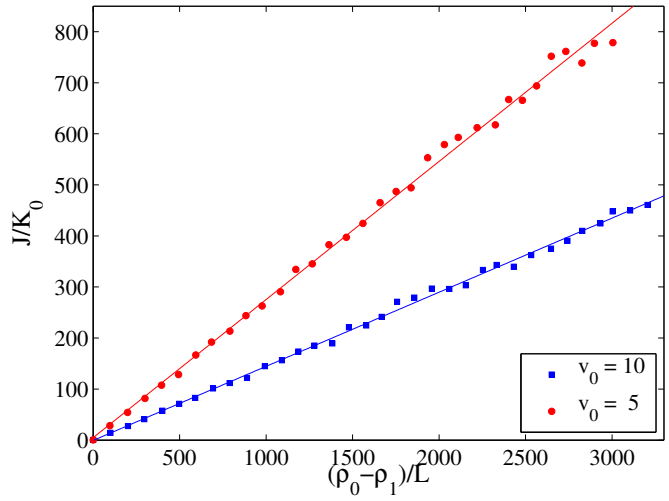

Figure 9: Flux against the concentration gradient for the complete dichotomic model for two different barrier heights. $f_0 = 50$, $\sigma_0 = 5$, $\rho_1 = 200$, where $f_i = \omega_i \gamma L^2 / k_B T$.

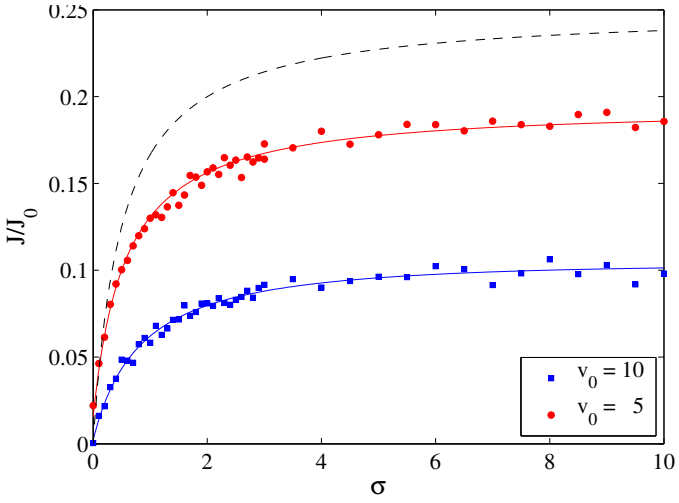

Figure 10: Normalized flux J/J_0 against σ for different simulation parameters, $f_0 = 100$. J_0 being the flux of free diffusion. See text for further explanation.

(circles). The black (dashed) curve is the zero order prediction, rescaled by one half for ease of view. It normally saturates at $J/J_0 = 1/2$.

Again, the results share the behavior with the zero order prediction. The

system still has the same dependence with the ATP concentration, but when it saturates it has a smaller flux value due to the presence of the barrier. Increasing the barrier height decreases the flux. It is important to note that the flux is only one order of magnitude smaller than the one expected from free diffusion, well in the limits of real biological channels.

Looking again at Fig. 10 we expect to obtain close to a linear relation if we plot the inverse of the flux against the inverse of σ (what biologists like to call a Lineweaver-Burk plot). The results of this new plot can be seen in Fig. 11.

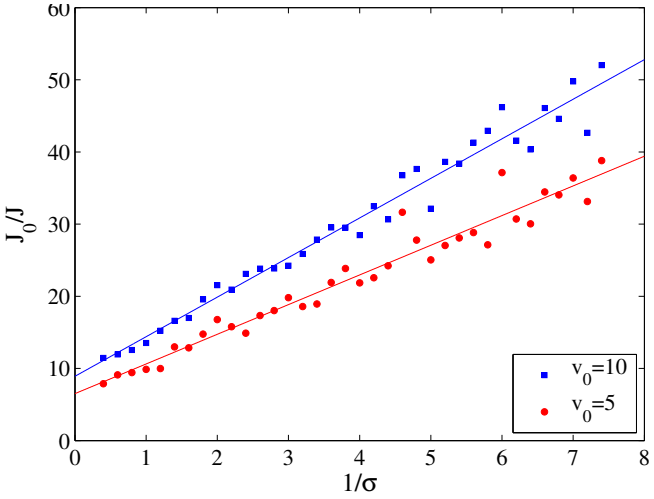

Figure 11: Lineweaver-Burk plot for $J(\sigma)$.

We can see how it fits quite well with a linear fit. From this plot we arrive to the conclusion that the flux dependence on the ATP concentration still follows a Michaelis-Menten law, but with new effective parameters that can be extracted form the linear regression.

In the complete dichotomic model we now have two parameters that cannot be compared with the zero order approximation. The first one being the barrier height V_0 and its effect, which can be seen in Fig. 12.

As expected, as the barrier increases the flux decreases, but now it does not decay to zero, as one would expect if there was only a barrier (the dashed line). It saturates, and its value depends on the parameters of the model. In the figure, the main difference between the blue and the red curves (squares and circles respectively) is the closing rate ω_0, being higher on the blue one. The green one (stars) has the same rate as the blue one, but with a much higher ATP concentration. We can again see that the ATP concentration has a big impact on the flux. Specially for high barriers.

The other new parameter is the closing rate ω_0. The zero order limit

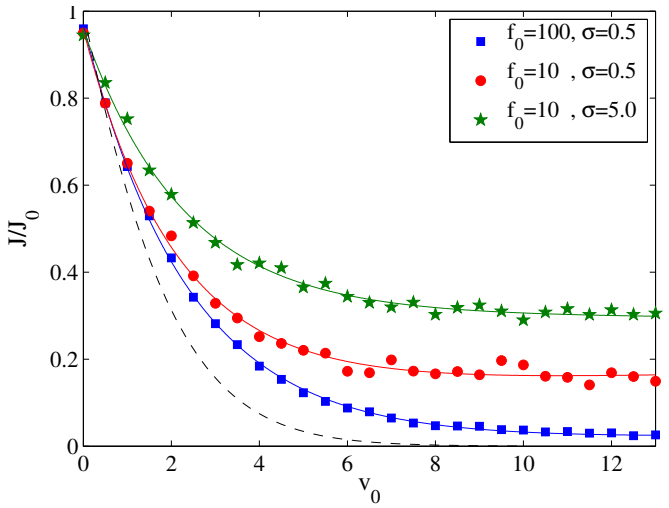

Figure 12: Normalized flux J/J_0 against V_0 for different simulation parameters. See text for further explanation

shows no dependence on it, but the complete model depends on it. The results of the simulation can be seen on Fig. 13.

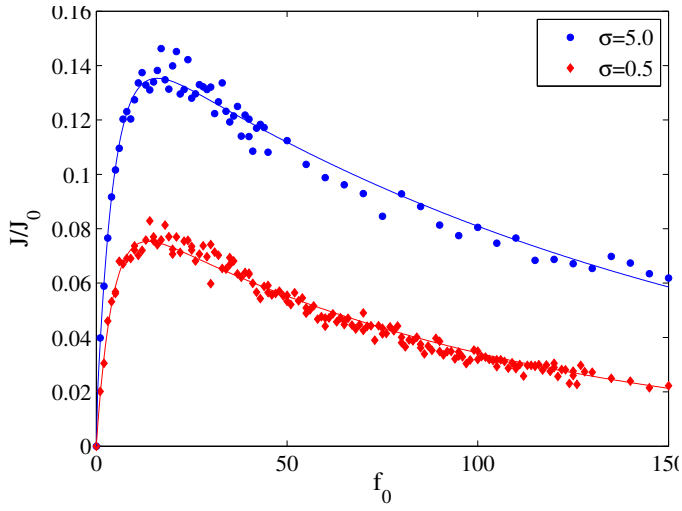

Figure 13: Normalized flux J/J_0 against closing rate f_0 for different simulation parameters, $v_0 = 5$.

Now we can appreciate how there is a maximum in the flux for a given closing rate f_0, and how it decays for very high rates. We can see that there is a small range of parameters for which the flux is maximized, and

the channel operates at its maximum efficiency. It seems that the position of the maximum does not depend on σ, and probably neither on the barrier height, but it is unclear at this point. The current working hypotheses is that the position of the maximum depends on the relationship between the closing rate and the characteristic diffusive length during that time.

We also expect biological channels to operate on this regime. Due to evolution, we expect these systems to have evolved until they work close to the most optimal regime.

5 Conclusions

The implementation of the dichotomic model has given us the ability to model the channel gating, which was lacking in the previous model. Also, the specific form used for the transition rates allows a direct connection to a more biochemical approach, either via Michaelis-Menten kinetics or through a different model, as will be seen in the next section.

One of the interesting results seen with this model is that now we can control the flux across the channel by just playing with the rates and the Michaelis constant, since the barrier height is not as important as in other models. The flux already saturates[6] for barriers that are only of the order of $10k_BT$.

Also important is the finding of a region where the flux is maximum for the closing rate ω_0. Since we have considered the parameters ω_0 to be intrinsic to the system, and depend mostly on things like its biochemical structure, we can predict that most biological channels will operate in this regime. Operating on this regime also implies a minimum in energy consumption, since one needs to open the channel less times to transport any amount of material. Due to this fact, we theorize that biological channels, being part of living beings, have evolved until archiving this regime.

6 Perspectives

The modeling of the transition rates via Michaelis-Menten kinetics allow us to characterize the energetics of the system. In connection with biological channels it gives us an upper limit to the input energy the system can receive, since it cannot be greater than the energy liberated by ATP hydrolysis. The next step would be to calculate the exact power input the channel receives when it closes, since in this model, the channel requires energy to close the gate, not to open it.

Also we have to take into account that we have used the Mass Action Law to model the transitions, which are only valid on the continuous limit,

[6] Does not really saturate, but becomes more or less independent of the barrier height.

and here we are dealing with just one channel, and maybe a very small amount of ATP. The problem could be extended by using a different kind of temporal distribution to model the transition probabilities [25].

Another future approach, is to fully study the dynamics of the system, the whole temporal evolution of the system, not just the study state. A comprehensive study of the temporal evolution of the channel between the closed and open transitions might give more clues on why is there a maximum on the flux for a specific set of parameters.

The framework used to model a channel driven by ATP hydrolysis can also be used to model other types of channels, like voltage-gated ones, but using a different procedure to model the transition rates.

6.1 Modeling a voltage-gated channel

Based on experimental evidence [4] we can use the dichotomic model to analyze voltage-gated channels, but now we need to use a different approach to characterize the transition rates. We still consider that the closing rate ω_0 is a characteristic time of the system, and has to do with the specific structure of the channel and conformational changes. Also, we know that if the channel is in equilibrium (for the transition rates), the probability ratio between open and closed states has to satisfy a relation of the form

$$\frac{P_0}{P_1} = e^{-\frac{\Delta G}{k_B T}} \equiv k, \tag{36}$$

where ΔG is the free energy difference between the open and closed states (in the grand canonical ensemble) of the system. But these probabilities are also related to the transition rates

$$\frac{P_0}{P_1} = \frac{\omega_1}{\omega_0}. \tag{37}$$

Also, following Kramer's work [26], we can consider that applying a voltage difference to the channel will modify the rates accordingly

$$\frac{P_0(V)}{P_1(V)} = e^{-\frac{\Delta G + qV}{k_B T}} = k e^{-\frac{qV}{k_B T}}, \tag{38}$$

where q is the typical membrane gating charge and V the applied voltage. Also, since $P_0 + P_1 = 1$ we obtain

$$P_1(V) = \frac{1}{1 + k e^{-\frac{qV}{k_B T}}}, \tag{39}$$

which matches very well experimental data [4].

Now that we have described the new rates we could proceed as we did with the ATP-driven channel and fully study the system.

References

[1] J. G. Orlandi. Biological transport: membrane channels, a white noise flashing ratchet model (`http://hdl.handle.net/2445/5801`). *Projectes finals del Màster Oficial de Biofísica*, 2008.

[2] David L. Nelson and Michael M. Cox. *Lehninger Principles of Biochemistry, Fourth Edition*. W. H. Freeman, April 2004.

[3] Harvey Lodish and James E. Darnell. *Molecular Cell Biology*. W.H.Freeman & Co Ltd, 5rev ed edition, August 2003.

[4] R P Hartshorne, B U Keller, J A Talvenheimo, W A Catterall, and M Montal. Functional reconstitution of the purified brain sodium channel in planar lipid bilayers. *Proceedings of the National Academy of Sciences of the United States of America*, 82(1):240–4, Jan 1985.

[5] Jeremy M. Berg, John L. Tymoczko, and Lubert Stryer. *Biochemistry, Fifth Edition : International Version*. W. H. Freeman, February 2002.

[6] David C Gadsby, Paola Vergani, and László Csanády. The abc protein turned chloride channel whose failure causes cystic fibrosis. *Nature*, 440(7083):477–83, Mar 2006.

[7] O Hamill, A Marty, E Neher, B Sakmann, and F Sigworth. Improved patch-clamp techniques for high-resolution current recording from cells and cell-free membrane patches. *Pflügers Archiv European Journal of Physiology*, 391(2):85–100, Aug 1981.

[8] Thomas M Fyles. Synthetic ion channels in bilayer membranes. *Chem. Soc. Rev.*, 36(2):335–47, Feb 2007.

[9] B Feringa. The art of building small: From molecular switches to molecular motors. *J. Org. Chem*, Jan 2007.

[10] E. M Purcell. Life at low reynolds number. *American Journal of Physics*, 45:3, Jan 1977.

[11] J Sancho, M Miguel, and D Dürr. Adiabatic elimination for systems of brownian particles with nonconstant damping coefficients. *Journal of Statistical Physics*, 28(2):291–305, Jun 1982.

[12] Crispin W. Gardiner. *Handbook of Stochastic Methods: for Physics, Chemistry and the Natural Sciences (Springer Series in Synergetics)*. Springer, 3rd ed. edition, April 2004.

[13] R Kupferman, G. A Pavliotis, and A. M Stuart. Itô versus stratonovich white-noise limits for systems with inertia and colored multiplicative noise. *Phys. Rev. E*, 70:36120, Sep 2004.

[14] A Gomez-Marin and J. M Sancho. Brownian pump powered by a white-noise flashing ratchet. *Phys. Rev. E*, 77:31108, Mar 2008.

[15] A. Gomez-Marin and J. M. Sancho. Two-state flashing molecular pump. Europhysics Letters (Pending publication), January 2009.

[16] V Shapiro and V Loginov. "formulae of differentiation" and their use for solving stochastic equations. *Physica A: Statistical and Theoretical Physics*, 91(3-4):563–574, 1978.

[17] L. Michaelis and M. L. Menten. Die kinetik der invertinwirkung. *Biochem. Z.*, 49:333, 1913.

[18] B Nadler, Z Schuss, and A Singer. Langevin trajectories between fixed concentrations. *Phys. Rev. Lett.*, 94:218101, Jun 2005.

[19] Rebecca L Honeycutt. Stochastic runge-kutta algorithms. i. white noise. *Physical Review A (Atomic*, 45:600, Jan 1992.

[20] A. C Brańka and D. M Heyes. Algorithms for brownian dynamics simulation. *Physical Review E (Statistical Physics*, 58:2611, Aug 1998.

[21] J. M Sancho, M San Miguel, S. L Katz, and J. D Gunton. Analytical and numerical studies of multiplicative noise. *Physical Review A (General Physics)*, 26:1589, Sep 1982.

[22] D T Gillespie. Exact stochastic simulation of coupled chemical reactions. *J. Phys. Chem.*, 81(25):2340–2361, Jan 1977.

[23] Darren J. Wilkinson. *Stochastic Modelling for Systems Biology*. Chapman & Hall/CRC, April 2006.

[24] G Marsaglia and W Tsang. The ziggurat method for generating random variables. *Journal of Statistical Software*, Jan 2000.

[25] Mahashweta Basu and P. K Mohanty. Stochastic modeling of single molecule michaelis menten kinetics. *arXiv*, physics.chem-ph, Jan 2009.

[26] P Hänggi, P Talkner, and M Borkovec. Reaction-rate theory: fifty years after kramers. *Reviews of Modern Physics*, Jan 1990.